Co-doped ceria: tendency towards ferromagnetism driven by oxygen vacancies

J. Phys.: Condens. Matter **22** (2010) 276002 (9pp) doi:10.1088/0953-8984/22/27/276002

Co-doped ceria: tendency towards ferromagnetism driven by oxygen vacancies

V Ferrari[1,2,4], **A M Llois**[1,2,3,4] **and V Vildosola**[1,2,4]

[1] Departamento de Física and INN, Centro Atómico Constituyentes, Comisión Nacional de Energía Atómica, Gral. Paz 1499, 1650 San Martín, Buenos Aires, Argentina
[2] Consejo Nacional de Investigaciones Científicas y Técnicas, C1033AAJ, Buenos Aires, Argentina
[3] Departamento de Física Juan José Giambiagi, Facultad de Ciencias Exactas y Naturales, Universidad de Buenos Aires, 1428 Buenos Aires, Argentina

Received 16 March 2010, in final form 28 April 2010
Published 17 June 2010
Online at stacks.iop.org/JPhysCM/22/276002

Abstract
We perform an electronic structure study for cerium oxide homogeneously doped with cobalt impurities, focusing on the role played by oxygen vacancies and structural relaxation. By means of full-potential *ab initio* methods, we explore the possibility of ferromagnetism as observed in recent experiments. Our results indicate that oxygen vacancies seem to be crucial for the appearance of a ferromagnetic alignment among Co impurities, obtaining an increasing tendency towards ferromagnetism with growing vacancy concentration. However, the estimated couplings cannot explain the experimentally observed room-temperature ferromagnetism. In this systematic study, we draw relevant conclusions regarding the location of the oxygen vacancies and the magnetic couplings involved. In particular, we find that oxygen vacancies tend to nucleate in the neighborhood of Co impurities and we get a remarkably strong ferromagnetic coupling between Co atoms and the Ce^{3+} neighboring ions. The calculated magnetic moments per cell depend on the degree of reduction, which could explain the wide spread in the magnetization values observed in the experiments.

(Some figures in this article are in colour only in the electronic version)

1. Introduction

The field of the so called diluted magnetic oxides (DMO) is currently being explored with the strong drive to find room-temperature (RT) ferromagnetic (FM) materials for possible technological applications [1]. DMO are experimentally obtained by doping the oxide matrix with a small amount of magnetic transition metal (TM) ions. This procedure may introduce ferromagnetism in otherwise nonmagnetic materials and open up the feasibility of applications that range from spintronics to magneto-optical devices.

Since the pioneering work of Dietl *et al* [2] predicting high Curie temperatures in various p-type semiconductors, RT ferromagnetism has been observed in various doped oxide hosts [3] with different TM ions and doping concentrations. Some DMO are FM insulators while others are semiconductors and, so far, there is no obvious link between the ferromagnetic behavior and the conduction properties. The samples are sensitive both to preparation methods and growth conditions and this observation supports the idea that ferromagnetism might be closely linked to defects and/or to the presence of oxygen vacancies. Interesting for spintronic applications are critical temperatures being far above room temperature.

Among DMO, Co-doped CeO_2 ($Co_xCe_{1-x}O_2$) has attracted particular interest due to its ferromagnetic behavior observed well above RT for low Co-doping concentration [4–8]. Moreover, ceria is a transparent and high dielectric constant rare-earth oxide, whose fluorite structure matches well with that of silicon. It retains this crystal structure, both under doping and upon the formation of oxygen vacancies, thus promising a good integrability for spintronic devices even for non-stoichiometric compounds. However, there is controversy among the experimental results regarding the critical temperatures and values of the magnetic moments as a function of

[4] These authors contributed equally to this work.

doping concentration. As a matter of fact, a wide range of magnetic moments has been reported [6, 5, 4, 8] and this has raised concerns about the intrinsic nature of the FM properties of these materials due, for example, to Co secondary phases, heterogeneities or even contamination.

The presence of oxygen vacancies has been considered as a possible factor affecting the FM response in the case of films [7] but it is not yet clear whether it induces Co clustering and/or promotes magnetic ordering. It has been recently argued that even without introducing magnetic impurities, the presence of oxygen vacancies in CeO_2 could stabilize ferromagnetism [9].

There is experimental evidence available, obtained using several techniques [10–14], indicating that the charge left behind by the oxygen vacancies gets localized near some Ce atoms driving the Ce^{4+} to Ce^{3+} reduction. In the case of undoped ceria, this localization has been previously addressed in [15–17]. The charge localization happens both in doped as well as in undoped $CeO_{2-\delta}$, and has to be properly taken into account since it might affect atomic relaxation and, in turn, the magnetic behavior. It is important to remark that in order to perform a theoretical study of the magnetic properties of Co-doped reduced ceria, it is critical to relax the crystal structure. In particular, without allowing atomic relaxations, it is not possible to account for the reduction of Ce (even within the DFT + U approach) leading consequently to a wrong picture of the magnetic interactions.

Previous *ab initio* DFT + U calculations have reported a detailed description of the relaxation processes in reduced ceria upon doping with transition metal atoms such as Zr [18] and Pd [19]. It results that relaxation is different in Zr-doped systems as compared to the Pd-doped ones, because the electronic distribution, which changes upon reduction [19], depends on the size and the chemical characteristics of the dopant.

Our goal in this paper is to explore the role played by oxygen vacancies on the magnetic properties of the bulk ceria matrix as a function of Co-doping concentration. We perform local density approximation (LSDA) + U calculations [20] in bulk unit cells with substitutional replacement of cobalt atoms into cerium sites, taking into account that the film thickness in the experiments is at the micrometer scale (see [5, 7, 8, 21]). In this work we consider, in the relaxation process, the presence of Ce^{3+} ions induced by reduction. We study the evolution of the magnetic interactions with the number of oxygen vacancies per Co atom, which (to the best of our knowledge) has not yet been reported for doped ceria.

We organize the paper as follows: in sections 2 and 3, the computational method is described. In sections 4 and 5, the effect of introducing oxygen vacancies in Co-doped ceria is studied. In section 6, the magnetic and electronic properties as a function of the dopant concentration and oxygen deficiency are explained and finally, in section 7, the results of this work are discussed.

2. Method of calculation

Density functional theory (DFT) [22] calculations are performed within the local density approximation (LDA) [23]. We use the full-potential augmented plane waves method as implemented in the Wien2k code [20], where the space is divided into muffin tin (MT) spheres around the atoms and an interstitial region. Plane waves are used to describe the region outside the spheres. The muffin tin radii used are $R_{MT}^{Co} = 1.9$ au, $R_{MT}^{O} = 1.6$ au, $R_{MT}^{Ce} = 2.3$ au. The number of plane waves in the interstitial region is set by the cut-off parameter $RK_{max} = 7$ (or six for the biggest cells), where R is the minimum R_{MT} in the corresponding cell. To attain the desired convergence precision, we use a $7 \times 7 \times 7$ k-mesh in the Brillouin zone for a Co-doping concentration of $x = 12.5\%$ and a $5 \times 5 \times 5$ mesh for $x = 6.25\%$.

The use of LDA might be questionable in the case of oxides with strong electronic correlations, due to its well known failure to properly describe the ground state properties. In the case of unreduced ceria, however, several theoretical works [24] have shown that LDA gives fairly good results for the ground state properties. It gives an insulator with a reasonable value for the band gap between the O p and Ce 5d states. Although the position of the unoccupied 4f states within this gap is not properly given by LDA, the ground state energetics of ceria is reasonably well described by this approach as there are no highly localized 4f states below the Fermi level in ceria [24]. In contrast, Ce_2O_3 (out of the scope of this work) is clearly not well described by LDA due to the strongly localized character of the 4f electron.

In the case of reduced ceria, where there is charge localization on the 4f states of some Ce ions (which we call Ce^{3+} ions), it is necessary to go beyond LDA. In this case, the structures are first allowed to relax taking these 4f electrons as core levels[5], until the forces on the atoms are below 1 mRyd au^{-1}. Then, the electronic structure of the fully relaxed supercell is obtained using the LSDA + U approach switching on the local Coulomb interaction in the Ce^{3+} ions [25] with $U_{eff} = U - J = 6$ eV [26]. The relaxation processes involved will be described in detail in section 5.

3. Supercell calculations

The crystal structure of CeO_2 is fluorite with an experimental lattice parameter of 5.411 Å. Each Ce^{4+} cation is coordinated to eight O^{2-} nearest neighbors and in turn, each O^{2-} is tetrahedrally coordinated to Ce^{4+} cations.

Previous theoretical results for doped ceria indicate very small changes in the lattice constants upon doping with different transition metals, while preserving the cubic symmetry [18, 19]. In particular, when doping with Zr, a 0.2% contraction in the lattice parameters is obtained [18] and a 0.04% reduction, when doping with Pd [19]. In both calculations the dopant concentration is 3%. Taking this fact into account, we consider the experimental lattice constants of unreduced CeO_2 for all the systems under study. However, as we are interested in understanding the effect of both magnetic

[5] We have checked the relaxation procedure with the 4f electrons of Cerium treated as core levels by relaxing the structure of undoped and reduced $CeO_{2-\delta}$ and comparing the results with the literature [19, 16]. We obtained a quantitative agreement regarding both the ionic relaxation and the electronic structure.

impurities and oxygen vacancies, it is essential to relax the internal atomic positions, as mentioned in section 2.

For a concentration of Co given by $x = 6.25\%$, we use a $2 \times 2 \times 2$ BCC-type supercell, and for $x = 12.5\%$, a $2 \times 2 \times 2$ FCC-type supercell. The supercells are built out of the conventional 12-atoms cubic unit cell of CeO_2 and are schematically shown in figure 1. For the unreduced compounds these supercells contain 48 and 24 atoms, respectively. The nearest neighbor distance between Co atoms is 9.37 Å in the BCC cell and 7.65 Å in the FCC one, so that these atoms can be safely considered as impurities.

For each concentration we study configurations with zero, one or two vacancies per Co impurity atom. When an oxygen vacancy is created in pure bulk CeO_2, two electrons are left in the system and the vacancy is surrounded by four next nearest neighbor Ce atoms. As mentioned before, several experimental results seem to indicate that these extra electrons occupy localized 4f states on two Ce sites. There are then, two types of Ce atoms: Ce^{4+} ions in a $4f^0$-like configuration and Ce^{3+} ions in a $4f^1$-like configuration that need to be considered theoretically (see for instance [15] and [27], and references therein).

When Co impurities are introduced the system gains in complexity. X-ray experiments suggest that in oxygen deficient samples the valence of Co is 2+ (see [14, 7, 8]). Regarding Ce, the presence of Ce^{3+} has been reported in [14, 7]. In particular, in [14], for a sample with a 4.5% Co concentration, the results seem to indicate that around 10% of the Ce atoms are Ce^{3+} while the others are Ce^{4+}.

Taking the above into account, in this work we consider a variety of situations, depending on the number of oxygen vacancies per impurity Co atom, as will be detailed in the following section. It is important to note that in these systems the percentage of oxygen vacancies can be as high as 20% without producing any structural transformation [14].

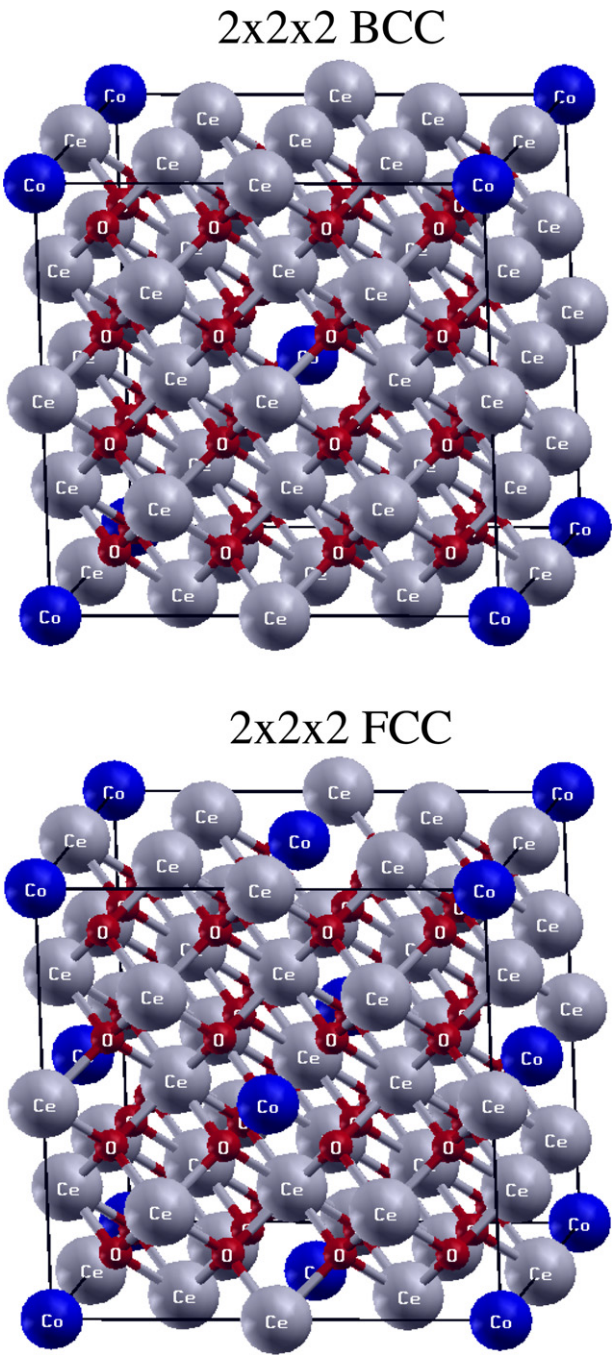

Figure 1. Supercells considered for two different Co-doping concentrations. Top: $2 \times 2 \times 2$ BCC-type supercell in which one of the 16 cerium sites is replaced by a Co atom. This supercell contains 48 atoms. Bottom: $2 \times 2 \times 2$ FCC supercell where one of the eight cerium sites is replaced by a Co atom. This is a 24 atom-supercell.

4. Location of the oxygen vacancies

The first question which arises when introducing vacancies into the Co–CeO_2 system relates to their location within the ceria matrix: what is energetically more favorable, to have oxygen vacancies close to or far from the Co impurities? To answer this question we first place one vacancy in a site nearest neighbor to a Co atom and relax the structure for the case $x = 12.5\%$. We then put the oxygen vacancy at the furthest distance from the Co impurity allowed by this concentration and, after relaxing the structure, we compare both results. In view of the experimental evidence mentioned in the previous section and the model suggested by Vodungbo *et al* [5], we consider that the extra electrons left behind by the vacancy migrate to the Co atoms, leaving all the Ce ions as Ce^{4+}, for both vacancy locations. The difference in energy between the two considered vacancy configurations is 0.55 eV per Co atom in favor of the vacancy being close to the impurity (see figure 2(b)).

We also consider a larger concentration of vacancies, namely, two per Co impurity atom and perform the calculations for $x = 6.25\%$. We take into account two possibilities: a configuration where the two oxygen vacancies are close to the Co atom as suggested in [5] (see the scheme in figure 2(c)) and a configuration where one oxygen vacancy is a nearest neighbor to the impurity while the other one is chosen to be at around 5 Å away both from the impurity as well as the other vacancy. Comparing the total energies of both configurations, we find that the two oxygen vacancies prefer to be close to the Co atom by 0.62 eV/Co atom.

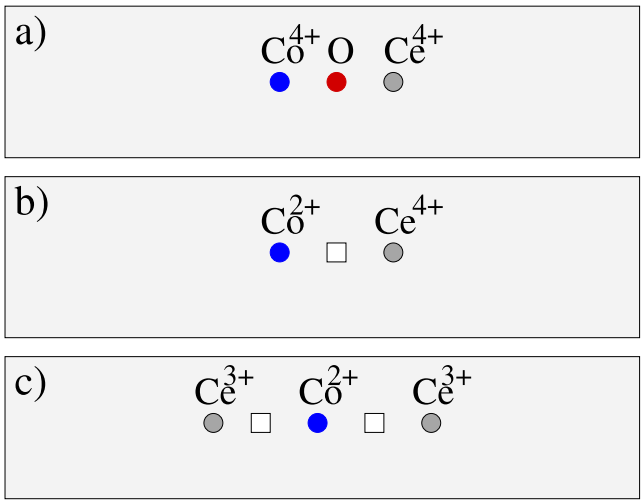

Figure 2. Schemes of the lowest energy configurations of oxygen vacancies within the ceria matrix for: (a) unreduced system. (b) One vacancy per Co atom. (c) Two vacancies per Co. The white square indicates an oxygen vacancy.

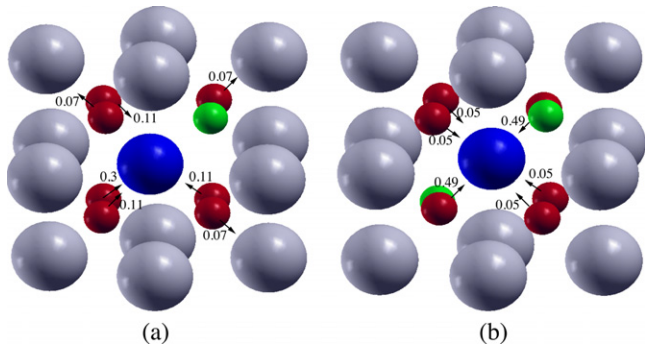

Figure 3. Schematic relaxation pattern around the impurity for $x = 12.5\%$. (a) One oxygen vacancy per Co atom (b) two oxygen vacancies per Co atom. The spheres show the atomic positions (up to second nearest neighbors of the impurity) after the relaxation has taken place. Red spheres denote oxygen atoms, the blue sphere is the cobalt atom, gray ones are cerium atoms and the green sphere denotes the vacancy site. The arrows indicate the direction of the movement due to relaxation and the numbers indicate the displacement in angstroms. See the text for details. (In black and white, big dark/big gray/small dark/small gray spheres denote Co/Ce/O/vacancy atoms.)

It is clear from these results that cobalt has a strong tendency to nucleate oxygen vacancies in ceria. In the following sections we discuss the relaxation process, the electronic structure and the magnetic couplings for the most favorable spacial distribution of vacancies.

5. Ionic relaxation

5.1. Zero oxygen vacancies

As discussed in section 4, for the doped system without oxygen vacancies, both Co and Ce are expected to be 4+ and therefore we use conventional LSDA calculations to relax the supercells for the two impurity concentrations considered. The obtained relaxations are qualitatively similar: the eight oxygen atoms which surround the impurity get symmetrically closer to it by 0.09 Å (for $x = 6.25\%$) and by 0.07 Å (for $x = 12.5\%$). Regarding the nearest cerium atoms, they move towards the impurity by around 0.04 Å for $x = 6.25\%$, while they do not relax due to symmetry reasons for the larger concentration considered.

5.2. One oxygen vacancy per Co atom

The valence configuration is depicted in figure 2(b). As there are no localized 4f electrons in the cell for this vacancy concentration, we again use conventional LSDA calculations and focus only on $x = 12.5\%$.

After relaxation, the seven oxygen atoms, which stay around the impurity after creating the vacancy, undergo a displacement of around 0.06 Å on average: one oxygen moves considerably towards Co (∼0.3 Å), three oxygen atoms get closer to it by ∼0.11 Å and the last three oxygen move outwards by ∼0.07 Å. Regarding the nearest neighbors of the vacancy, the nearest three Ce ions and the Co impurity move outwards with respect to it (the Ce atoms displace by 0.1 Å and the Co atom by 0.28 Å) while the six nearest neighbor oxygen atoms move towards the vacancy by 0.15 Å on average. Figure 3 shows an schematic picture of the relaxation pattern.

5.3. Two oxygen vacancies per Co atom

We consider the most stable vacancy location, namely, the two vacancies being near the impurity atom. As mentioned above, in this case, the extra electronic charge left behind by the vacancy, localizes at two Ce atoms, which are nearest neighbors to Co.

The six oxygen atoms surrounding the transition metal impurity relax towards it. For $x = 6.25\%$, two of them displace by ∼0.27 Å while the other four do so by ∼0.15 Å. The oxygen atoms which are nearest neighbors to the Ce^{3+} ions move away from them, on average by about 0.1 Å. This expansion of all oxygen atoms around the Ce^{3+} o connected with the Coulomb repulsion due to the extra charge localized at that Ce site. In contrast, this is not observed around the Ce^{4+} ions, where some of the nearest neighbor oxygen atoms get closer to these ions while others move away, but without undergoing a net expansion of the oxygen-cloud. Qualitatively similar behavior is obtained for atomic relaxations in the $x = 12.5\%$ case, with more pronounced displacements (see figure 3). It is clear that the introduction of vacancies produces an important rearrangement of the structure.

5.4. Comparison with other dopants

It is interesting to compare the results obtained when doping with Co with those appearing in the literature for other dopants such as Zr or Pd. The available data include cases considering just one vacancy per impurity [18, 19].

For unreduced ceria, relaxation in the presence of Zr impurities is similar to that of Co: the 8 nearest neighbor oxygen atoms and the three nearest Ce^{4+} ions move towards the impurity by ∼0.1 Å and ∼0.036 Å, respectively [18]. This

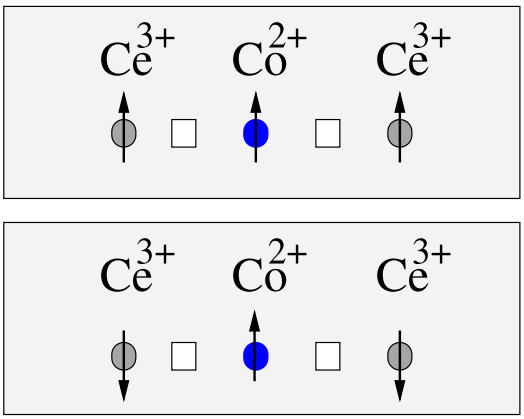

Figure 4. Scheme of the two configurations considered for calculating the magnetic coupling between Co and Ce^{3+} ions (top, FM. Bottom, AFM). The FM configuration is favored by an energy difference of 120 meV/Co atom.

is due to the fact that Zr and Co have smaller atomic radii than the Ce^{4+} ion. When doping with Pd, which has an atomic radius similar to the ionic radius of Ce^{4+}, the displacements towards the impurity are smaller than in the case of Zr and Co [19].

In the presence of one oxygen vacancy, relaxation for Co-doping resembles neither the Pd nor the Zr dopant cases. Co and Zr move away from the vacancy while Pd moves towards it. All nearest neighbor oxygen atoms get closer to the vacancy when the dopants are Co and Pd. In the case of Zr, most of those oxygen ions move towards the vacancy, except for one oxygen that moves away from it [18].

The above mentioned differences in the relaxation processes might be due to different reasons: in the case of Zr-doping, the charge left behind by the vacancy localizes on two neighboring Ce atoms, while for Pd and Co it localizes both at the impurity site and at its nearest neighbor oxygen atoms. When doping with Pd, the difference in relaxation might be due to the different size of the dopant atomic radii.

6. Magnetic and electronic properties of ceria as a function of Co-doping and reduction

6.1. Magnetic coupling between cobalt and Ce^{3+} ions

Before going into the analysis of the evolution of the electronic and magnetic properties of ceria as a function of dopant and vacancy concentration, it is interesting to determine the nature of the magnetic coupling between Ce^{3+} and Co. From the above discussion, it is clear that this coupling takes place when two vacancies per Co are present. To gain an insight into this problem, we consider the case of $x = 12.5\%$ to compare the energies of FM and AFM spin-alignments of Ce^{3+} with respect to Co, as depicted in figure 4. The energy difference between these configurations is 120 meV/Co atom in favor of the FM alignment. Cobalt and Ce^{3+} ions then show a strong ferromagnetic coupling.

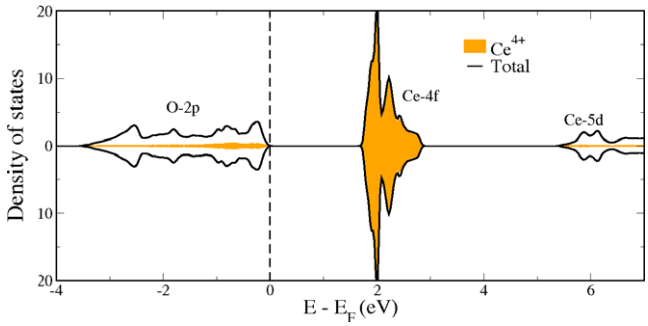

Figure 5. Total density of states for pure CeO_2 (black line) and partial density of states for Ce (orange). The units on the y-axis are (states eV^{-1}). Top: up-spin channel. Bottom: down-spin channel (upside-down).

Table 1. $\Delta E = E_{FM} - E_{AF}$, energy difference per Co ion (in meV) between FM and AF solutions, to estimate the magnetic coupling between Co atoms, for different cobalt concentration x and number of vacancies.

Case	ΔE ($x = 6.25\%$)	ΔE ($x = 12.5\%$)
0 vac	+0.4	+2.5
1 vac	0.0	−0.5
2 vac	−3.1	−12.5

6.2. Electronic structure and magnetic coupling among dopants

Pure CeO_2, without impurities or oxygen vacancies, is a nonmagnetic insulator. The occupied bands are mainly of O 2p character and the unoccupied ones are mostly of Ce 4f character (see figure 5). When impurities are introduced in the unreduced system, defect states appear due to majority and minority contributions coming from the d states of the substitutional Co atoms. For both impurity concentrations, and no oxygen vacancies, the magnetic coupling among Co ions is slightly antiferromagnetic. In table 1, we show the energy differences among FM and AFM configurations, $\Delta = E_{FM} - E_{AF}$ for[6] both Co concentrations and different number of vacancies per Co.

When oxygen vacancies are introduced, a tendency towards FM Co–Co coupling appears. The energy difference ΔE changes sign, thus favoring a growing FM alignment, which increases with both vacancy and Co concentration. For the largest Co concentration, the vacancy-induced ferromagnetic Co–Co coupling is clearly established.

Experimental evidence seems to suggest that there are no metallic Co clusters or secondary phase formation in Co-doped ceria [6, 4]. In this work, assuming that Co impurities are diluted and homogeneously distributed within the ceria matrix, a tendency towards ferromagnetism is obtained. This tendency increases with oxygen deficiency. However, the energy differences obtained cannot explain the high Curie temperatures observed in the experiments. Thus, the underlying mechanism for the observed room-temperature ferromagnetism remains unclear.

[6] To compute $\Delta E = E_{FM} - E_{AF}$, the total energy calculations are performed for unit cells twice as large as the ones described in section 3.

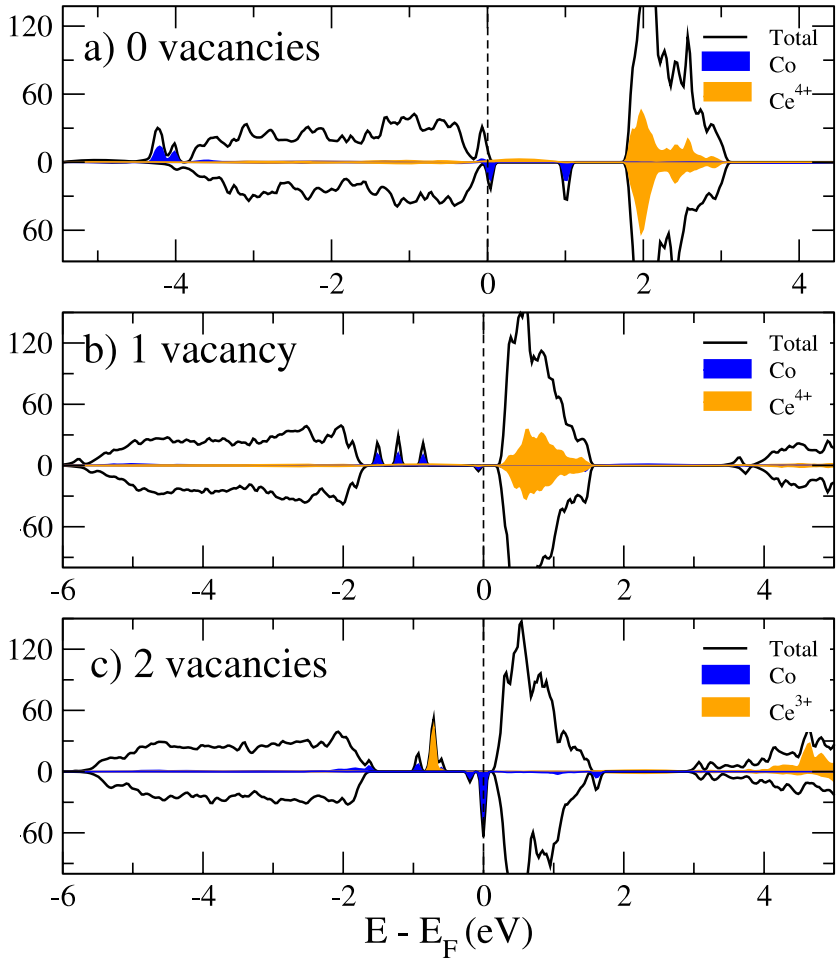

Figure 6. Density of states for $Ce_{1-x}Co_xO_{2-\delta}$ with $x = 6.25\%$ for (a) unreduced system ($\delta = 0$), (b) one vacancy per Co ($\delta = 0.0625$), and (c) two vacancies per Co ($\delta = 0.125$). Total DOS (black line), partial DOS for cobalt (blue) and cerium (orange). In (a) and (b), there is no charge localization on any Ce site. In (c) the partial DOS of a Ce^{3+} is shown. Units and spin channels as in figure 5.

To compare the effect that the introduction of vacancies has on the electronic structure of doped ceria, we show the densities of states corresponding to the FM solutions. As can be observed in figures 6(a) and 7(a), for the two unreduced Co concentrations considered here, two broad impurity peaks of O p character develop at the bottom of the majority valence band. The most important contribution to the peak appearing at the top of the majority valence band comes from the oxygen atoms which are nearest neighbors of the Co impurities. The orbitals of these oxygen atoms are magnetically polarized due to hybridization with the Co d impurity orbitals. Two localized minority impurity peaks lie in the gap of ceria. For both Co concentrations, the Fermi level falls within the first minority peak, which lies at the top of the oxygen minority p band. The second and unoccupied minority impurity peak appears well inside the original gap of ceria, far from the band edges.

In order to better follow the evolution of the impurity peaks with the introduction of vacancies, we show in figure 8 the projected local densities of states on Co for $x = 6.25\%$. The trends are similar for $x = 12.5\%$, with more delocalized impurity bands due to larger Co–Co hybridization.

When oxygen vacancies are introduced, Co^{4+} reduces to Co^{2+}. In figures 6(b), (c), 7(b) and (c), the corresponding total densities of states and the Co local densities of states are shown. Due to the Coulomb repulsion the large spectral weight of Co d character, originally lying at the bottom of the majority valence band, develops into two new majority peaks, which can be observed above this band. There are now three majority Co impurity peaks lying below the Fermi level and above the valence band in these reduced configurations for the two Co concentrations considered.

When two oxygen vacancies per Co are present, the extra charge, which localizes on two Ce^{3+} sites, gives rise to the occupied majority peak of 4f character which can be observed in figures 6(c) and 7(c).

6.3. Evolution of the magnetic moments

In the non reduced impurity systems, the total magnetic moment of the FM cells is mainly due to the polarization of Co and its nearest neighbor oxygen atoms. The AFM solution shows a distribution of the magnetic polarization among the atoms which is not different from the one obtained for the FM solution. The hybridization effects are, namely, very local. The eight nearest neighbor oxygen atoms of Co become

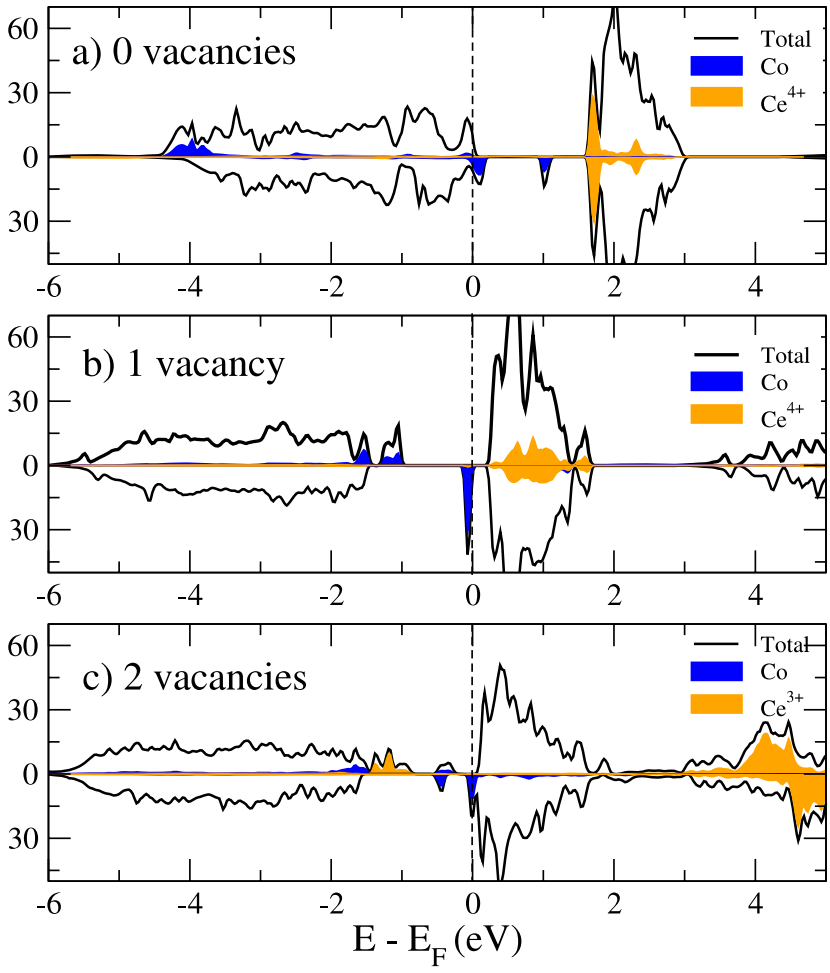

Figure 7. Density of states for $Ce_{1-x}Co_xO_{2-\delta}$ with $x = 12.5\%$ for (a) unreduced system ($\delta = 0$), (b) one vacancy per Co ($\delta = 0.125$), and (c) two vacancies per Co ($\delta = 0.25$). Total DOS (black line), partial DOS for cobalt (blue) and cerium (orange). In (a) and (b), there is no charge localization on any Ce site. In (c) the partial DOS of a Ce^{3+} is shown.

Table 2. Magnetic moments (in μ_B) for $x = 6.25\%$: μ_O^{nn} means the sum of the magnetic moments of all oxygen atoms nearest neighbor to cobalt. $\mu(Co + O^{nn})$ means the magnetic moment of the cloud formed by the Co and its nearest neighbors. $\mu(Ce')$ is the one corresponding to a cerium atom close to the vacancy. For the two vacancy case, there are two reduced Ce per cobalt.

Case	μ_T	μ_{Co}	μ_O^{nn}	$\mu(Co + O^{nn})$	$\mu(Ce')$
0 vac	4.76	2.94	1.28	4.22	0.04
1 vac	3.00	2.50	0.42	2.92	−0.17
2 vac	5.00	2.49	0.37	2.86	0.95

Table 3. Same caption as table 2, for $x = 12.5\%$.

Case	μ_T	μ_{Co}	μ_O^{nn}	$\mu(Co + O^{nn})$	$\mu(Ce')$
0 vac	4.60	2.90	1.28	4.18	0.04
1 vac	3.00	2.50	0.40	2.90	−0.03
2 vac	5.00	2.41	0.40	2.81	0.99

ferromagnetically polarized with respect to the impurity, for both Co concentrations. See tables 2 and 3.

When we introduce one vacancy, the two extra electrons which are left behind give rise to a decrease in the total magnetic moment of the ferromagnetic cell. The total moment goes from 4.76 μ_B (for $x = 6.25\%$) and 4.60 μ_B (for $x = 12.5\%$) to 3 μ_B. This decrease in the value of the magnetic moment per Co atom of almost 2 μ_B points towards an effective Co valence which goes from 4+ to 2+. The extra charge left behind by the oxygen vacancy localizes, then, in the electronic cloud surrounding the transition metal ion, which is covalently shared by this ion and the seven remaining nearest neighbor oxygen atoms.

Finally, when there are two vacancies per Co, the magnetic moment per magnetic ion is 5 μ_B, for both Co concentrations. From the four extra electrons per Co atom left behind by the vacancies, two contribute to decrease the magnetic moment of the cloud formed by Co and its neighboring oxygen atoms with respect to the unreduced situation. The other two electrons get localized on two Ce^{3+} sites close to the vacancies, giving rise to the increase in 2 μ_B of the magnetic moment of the cell per Co atom which goes from 3 to 5 μ_B. See tables 2 and 3.

The values of the total magnetic moments of the ferromagnetic cells also reveal that the introduction of

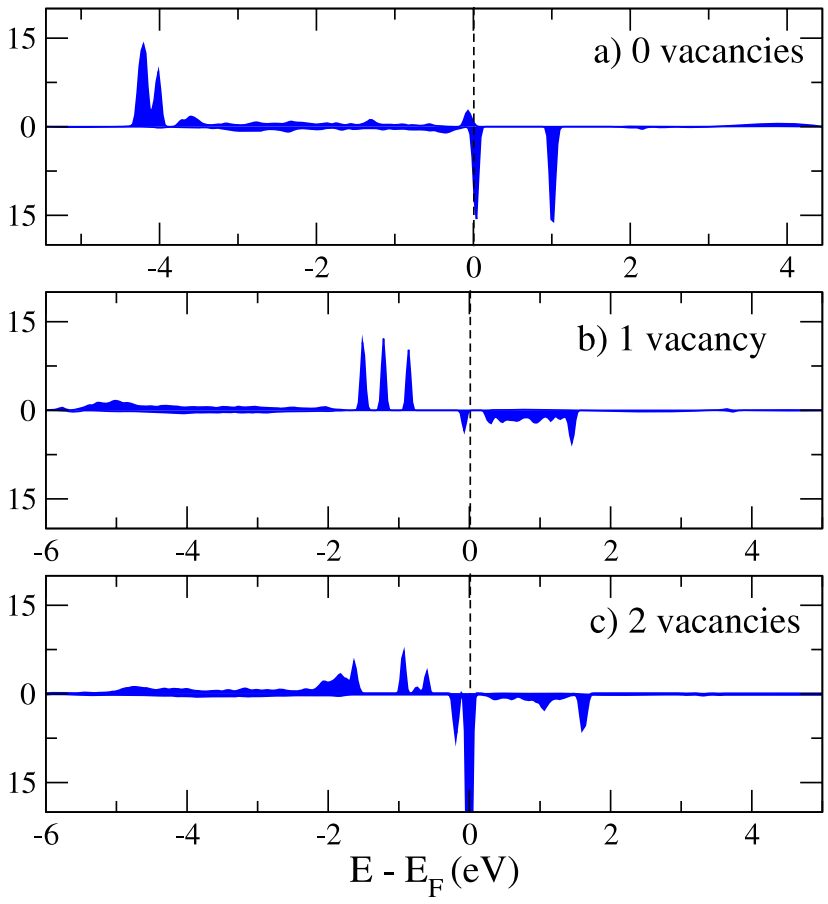

Figure 8. Local density of states on the Co impurity site, with increasing oxygen vacancy concentration for Co concentration $x = 6.25\%$. (a) Without vacancies, (b) one vacancy per Co, (c) two vacancies per Co. Units and spin channels as in figure 5.

vacancies changes the band character of the doped systems. The unreduced impurity systems show a non integer cell magnetic moment, characteristic of a metallic-like band structure, while the introduction of vacancies gives rise to half-metallic-like features, as for instance the integer value of the total cell spin moments.

It is interesting to remark, again, that the total magnetic moment per cell strongly depends on the degree of reduction. This might explain the wide spread in the magnetization values obtained in the experiments as reported in the literature [6, 5, 4, 8].

7. Discussion and conclusions

In this work we have studied the effect of oxygen vacancies on the magnetic and electronic properties of Co-doped ceria. We have shown that the introduction of oxygen vacancies is essential to drive the ferromagnetic coupling among the dopant impurities. Actually, in the absence of vacancies there is a slight tendency towards an antiferromagnetic coupling that changes towards a ferromagnetic one when the vacancy concentration increases.

For two vacancies per Co, part of the left behind charge localizes on Ce ions sitting in the vicinity of the impurity, turning them into magnetic Ce^{3+} ions. We find that the magnetic coupling among the Co impurities and the Ce^{3+} ions is strongly ferromagnetic. This coupling provides a large magnetic moment, localized close to the impurity.

Even if Co impurities in unreduced ceria show large local magnetic moments, the interaction among impurities is small for the two dopant concentrations studied. The same can be said about the systems with only one vacancy per impurity atom. The ferromagnetic coupling among impurities in the presence of two vacancies per Co increases when going from an impurity concentration of 6.25% to 12.5%.

We conclude that, although there is a clear tendency towards ferromagnetism in Co-doped ceria when oxygen vacancies are present, the obtained FM couplings cannot explain the high Curie temperatures observed in the experiments. On the other hand, the large values of the magnetic moments per Co atom observed can be understood if the Co impurities, the vacancies and the nearest Ce^{3+} ions build complexes of the type considered in this work. To understand the simultaneous appearance of the two phenomena, namely Curie temperatures above RT and a wide spread in the large values of the magnetic moments per Co dopant, it might be necessary to consider eventual inhomogeneities and/or to introduce other magnetic interaction mechanisms beyond the exchange interactions taken into account within the framework of these DFT calculations.

Acknowledgments

We are grateful to V Etgens and F Vidal for motivating these calculations and giving us their experimental insight. We acknowledge useful discussions with R Weht, V Ganduglia-Pirovano, J Milano, M Weissmann and R Faccio. In particular, we are indebted to R Weht regarding the calculation of the magnetic coupling for the supercell-BCC system. This work was funded by CONICET, ANPCyT and UBA (Argentina) through grants PIP-CONICET-6016, UBACYT-X123, PICT06-157, PICT06-1765, PICT05-33304 and PIP-CONICET-00038.

References

[1] Dietl T 2007 *J. Phys.: Condens. Matter* **19** 165204
[2] Dietl T, Ohno H, Matsukura F, Cibert J and Ferrand D 2000 *Science* **287** 1019
[3] Chambers S A 2006 *Surf. Sci. Rep.* **61** 345–81
[4] Tiwari A, Bhosle V M, Ramachandran S, Sudhakar N, Narayan J, Budak S and Gupta A 2006 *Appl. Phys. Lett.* **88** 142511
[5] Vodungbo B, Zheng Y, Vidal F, Demaille D, Etgens V H and Mosca D H 2007 *Appl. Phys. Lett.* **90** 062510
[6] Fernandes V, Klein J J, Mattoso N, Mosca D H, Silveira E, Ribeiro E, Schreiner W H, Varalda J and de Oliveira A J A 2007 *Phys. Rev.* B **75** 121304(R)
[7] Song Y-Q, Zhang H-W, Wen Q-Y, Peng L and Xiao J Q 2008 *J. Phys.: Condens. Matter* **20** 255210
[8] Wen Q-Y, Zhang H-W, Song Y-Q, Yang Q-H, Zhu H and Xiao J Q 2007 *J. Phys.: Condens. Matter* **19** 246205
[9] Han X, Lee J and Yoo H-I 2009 *Phys. Rev.* B **79** 100403(R)
[10] Henderson M A, Perkins C L, Engelhard M H, Thevuthasan S and Peden C H F 2003 *Surf. Sci.* **526** 1
[11] Liu G, Rodriguez J A, Hrbek J, Dvorak J and Peden C H F 2001 *J. Phys. Chem.* B **105** 7762
[12] Mullins D R, Overbury S H and Huntley D R 1998 *Surf. Sci.* **409** 327
[13] Esch F, Fabris S, Zhou L, Montini T, Africh C, Fornasiero P, Comelli G and Rosei R 2005 *Science* **309** 752
[14] Vodungbo B, Vidal F, Zheng Y, Marangolo M, Demaille D, Etgens V H, Varalda J, de Oliveira A J A, Maccherozzi F and Panaccione G 2008 *J. Phys.: Condens. Matter* **20** 125222
[15] Skorodumova N V, Simak S I, Lundqvist B I, Abrikosov I A and Johansson B 2002 *Phys. Rev. Lett.* **89** 166601
[16] Fabris S, de Gironcoli S, Baroni S, Vicario G and Balducci G 2005 *Phys. Rev.* B **71** 041102
[17] Verónica Ganduglia-Pirovano M, DaSilva J L F and Sauer J 2009 *Phys. Rev. Lett.* **102** 026101
[18] Yang Z, Woo T K and Hermansson K 2006 *J. Chem. Phys.* **124** 224704
[19] Yang Z, Luo G, Lu Z and Hermansson K 2007 *J. Chem. Phys.* **127** 074704
[20] Blaha P, Schwarz K, Madsen G, Kvasnicka D and Luitz J 2002 *WIEN2k, An Augmented Plane Wave + Local Orbitals Program for Calculating Crystal Properties* ISBN 3-9501031-1-2
[21] Bi L, Kim H-S, Dionne G F, Speakman S A, Bono D and Ross C A 2008 *J. Appl. Phys.* **103** 07D138
[22] Hohenberg P and Kohn W 1964 *Phys. Rev.* **136** B864–71
[23] Perdew J P and Wang Y 1992 *Phys. Rev.* B **45** 13244
[24] DaSilva J L F, Verónica Ganduglia-Pirovano M, Sauer J, Bayer V and Kresse G 2007 *Phys. Rev.* B **75** 045121
[25] Anisimov V I, Solovyev I V, Korotin M A, Czyzyk M T and Sawatzky G A 1993 *Phys. Rev.* B **48** 16929
[26] Andersson D A, Simak S I, Johansson B, Abrikosov I A and Skorodumova N V 2007 *Phys. Rev.* B **75** 035109
[27] Ganduglia-Pirovano M V, Hofmann A and Sauer J 2007 *Surf. Sci. Rep.* **62** 219